Insulin-like growth factor 1 treatment extends longevity in a mouse model of human premature aging by restoring somatotroph axis function

Guillermo Mariño[a,1], Alejandro P. Ugalde[a,1], Álvaro F. Fernández[a], Fernando G. Osorio[a], Antonio Fueyo[b], José M. P. Freije[a], and Carlos López-Otín[a,2]

[a]Departamento de Bioquímica y Biología Molecular and [b]Biología Funcional, Facultad de Medicina, Instituto Universitario de Oncología, Universidad de Oviedo, 33006 Oviedo, Spain

Edited by Cynthia Kenyon, University of California, San Francisco, CA, and approved August 4, 2010 (received for review March 2, 2010)

Zmpste24 (also called FACE-1) is a metalloproteinase involved in the maturation of lamin A, an essential component of the nuclear envelope. Zmpste24-deficient mice exhibit multiple defects that phenocopy human accelerated aging processes such as Hutchinson–Gilford progeria syndrome. In this work, we report that progeroid *Zmpste24*$^{-/-}$ mice present profound transcriptional alterations in genes that regulate the somatotroph axis, together with extremely high circulating levels of growth hormone (GH) and a drastic reduction in plasma insulin-like growth factor 1 (IGF-1). We also show that recombinant IGF-1 treatment restores the proper balance between IGF-1 and GH in *Zmpste24*$^{-/-}$ mice, delays the onset of many progeroid features, and significantly extends the lifespan of these progeroid animals. Our findings highlight the importance of IGF/GH balance in longevity and may be of therapeutic interest for devastating human progeroid syndromes associated with nuclear envelope abnormalities.

laminopathy | microRNA | progeria | protease | cancer

Aging is a natural process that affects most biological functions and appears to be a consequence of the accumulative action of different types of stressors. Among these, oxidative damage, telomere attrition, and the decline of DNA repair and protein turnover systems are thought to be major causes of aging (1, 2). Over the last few years, our knowledge of the molecular basis of aging has gained mechanistic insight from studies on progeroid syndromes in which features of human aging are manifested precociously or in an exacerbated form. The vast majority of progeroid syndromes are a consequence of inefficient DNA repair mechanisms or defective nuclear envelope assembly, which ultimately lead to DNA damage accumulation and chromosome instability (3). Thus, mutations in the gene encoding lamin A (an essential component of the nuclear envelope) or in *Zmpste24* (encoding a metalloproteinase involved in the maturation of lamin A) are responsible for several devastating human progeroid syndromes, including Hutchinson–Gilford progeria, atypical Werner syndrome, restrictive dermopathy, and mandibuloacral dysplasia (3–7). The elucidation of the molecular mechanisms underlying these diseases has been facilitated by the generation and analysis of *Lmna*- and *Zmpste24*-deficient mice, which exhibit profound nuclear architecture abnormalities and multiple histopathological defects that phenocopy human progeroid syndromes (8–12).

In recent years, somatotroph [i.e., growth hormone (GH)/insulin-like growth factor 1 (IGF-1)] signaling has been identified as a major regulator of longevity from nematodes to man (13). Paradoxically, studies have shown that reduced somatotroph signaling is a common feature of both long-lived model organisms and progeroid mice harboring alterations in DNA-repair mechanisms (14, 15). However, to date no studies have been undertaken to evaluate whether the down-regulation of IGF-1 signaling observed in premature aging is a beneficial adaptive response or a detrimental event that directly contributes to the development of progeroid features. In the present work, we report that *Zmpste24*$^{-/-}$ mice, which constitute an appropriate murine model of Hutchinson–Gilford progeria, demonstrate a clear dysregulation of somatotroph axis signaling. In addition, we show that this alteration is detrimental, given that *Zmpste24*$^{-/-}$ mice treated with recombinant IGF-1 show a clear amelioration of progeroid features and significantly extended longevity compared with untreated *Zmpste24*$^{-/-}$ mice.

Results

To gain insight into the alterations associated with the premature aging phenotype observed in *Zmpste24*$^{-/-}$ mice, and considering the increasing evidence for the importance of somatotroph axis regulation in longevity, we analyzed IGF-1 plasma levels in 1-, 2- and 4-mo-old progeroid mice. As shown in Fig. 1*A*, 1-mo-old *Zmpste24*$^{-/-}$ mice—which do not yet exhibit any obvious progeroid features—already demonstrate a significant reduction in circulating IGF-1 levels, which progressively declines as the mice prematurely age. Given that IGF-1 synthesis is regulated mainly by circulating GH, we measured plasma GH concentration in the same *Zmpste24*$^{-/-}$ mice. As shown in Fig. 1*A*, we found that although 1-mo-old mutant mice show circulating GH levels comparable to those from age-matched WT littermates, 2- and 4-mo-old progeroid mice show a drastic, progressive increase in circulating GH (~5- and 11-fold, respectively). To test whether the somatotroph alterations of mutant mice could be simply a consequence of their premature aging, we measured plasma levels of IGF and GH in 1- and 2-y-old WT mice from the same genetic background. As shown in Fig. 1*A*, the alterations in circulating IGF-1 and GH levels seen in *Zmpste24*$^{-/-}$ mice were not observed in aged WT controls. This suggests that the somatotroph deregulation of progeroid mice is not just a secondary consequence of their premature aging, but rather an early pathological situation that could contribute to the development of the progeroid phenotype and reduced lifespan characteristic of *Zmpste24*$^{-/-}$ mice. Reduced IGF-1 and increased circulating GH are common features of GH resistance, also known as Laron syndrome (LS) (16). Interestingly, some pathological features of LS are also found among the complex phenotypic manifestations of these progeroid mice. Both *Zmpste24*$^{-/-}$ mice and LS patients have reduced muscle development, strength, and endurance, as well as decreased bone mineral density, and both exhibit alopecia, skin atrophy, and hypoglycemia (8, 16, 17).

As a first step to elucidating the molecular determinants for the GH/IGF-1 axis alteration observed in *Zmpste24*$^{-/-}$ mice, we performed a detailed analysis of our previously reported transcriptome data of liver from these progeroid mice (9). In addition to the reported

Author contributions: G.M., A.P.U., J.M.P.F., and C.L.-O. designed research; G.M., A.P.U., Á.F.F., F.G.O., and A.F. performed research; G.M., A.P.U., F.G.O., A.F., J.M.P.F., and C.L.-O. analyzed data; and G.M., A.P.U., and C.L.-O. wrote the paper.

The authors declare no conflict of interest.

This article is a PNAS Direct Submission.

[1]G.M. and A.P.U. contributed equally to this work.

[2]To whom correspondence should be addressed. E-mail: clo@uniovi.es.

This article contains supporting information online at www.pnas.org/lookup/suppl/doi:10.1073/pnas.1002696107/-/DCSupplemental.

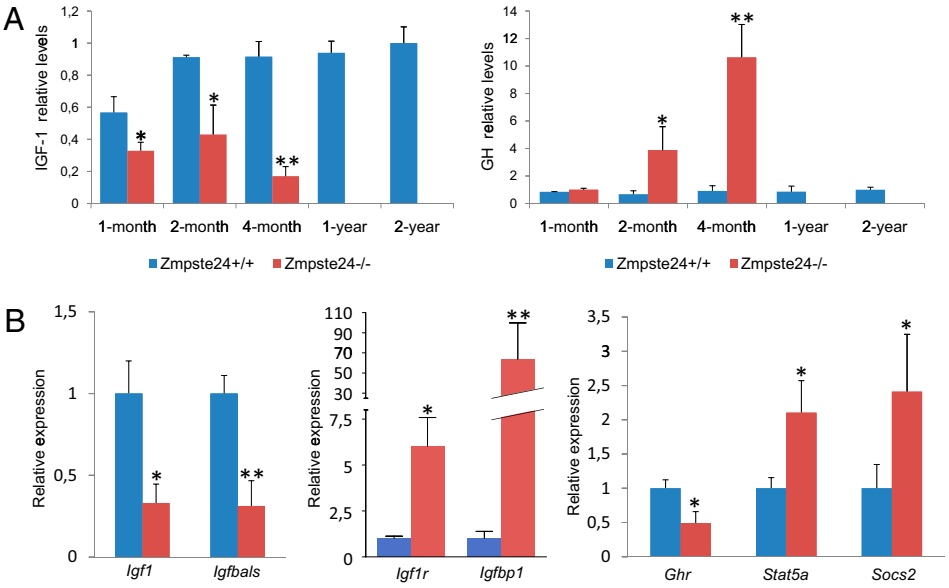

Fig. 1. Somatotroph axis alterations in *Zmpste24*$^{-/-}$ mice. (*A*) Plasma concentration of IGF-1 (*Left*) and GH (*Right*) in WT mice (blue bars) and *Zmpste24*$^{-/-}$ mice (red bars). The depicted values indicate a progressive reduction of circulating IGF-1 together with a progressive increase of plasma GH in *Zmpste24*$^{-/-}$ mice. (*B*) qPCR evaluation of mRNA levels of key genes for somatotroph axis in liver. Blue bars represent WT mice, whereas red bars correspond to *Zmpste24*$^{-/-}$ mice. Error bars indicate the SEM between replicates. At least eight WT and eight mutant animals were used for each assay. *$P <$ 0.05; **$P < 0.005$, one-tailed *t* test.

changes in glucose and lipid metabolism genes (17, 18) and the marked up-regulation of components of the p53-signaling pathway (9), we observed that many genes involved in somatotroph axis signaling were transcriptionally altered in the liver of *Zmpste24*$^{-/-}$ mice (Table 1). To further evaluate these results, we performed a quantitative PCR (qPCR) analysis of selected GH/IGF-1 axis genes in liver samples from *Zmpste24*$^{-/-}$ mice. As shown in Fig. 1*B*, mRNA levels of *IGF-1* were significantly lower in mutant mice compared with their control littermates. Similarly, mutant mice showed reduced levels of *Igfals* transcripts encoding the IGF-binding protein acid labile subunit, which has been associated with reduced levels of circulating IGF-1 in vivo (19, 20). In contrast, *Igfbp1*, the up-regulation of which is also associated with a reduced effective IGF-1 concentration (21), was transcriptionally up-regulated in *Zmpste24*$^{-/-}$ mice. Likewise, *IGF-1r* (IGF-1 receptor) mRNA levels were markedly increased in mutant mice, possibly reflecting a compensatory attempt to amplify the IGF-1 signaling. We also found alterations in genes involved in GH-mediated signaling. In fact, although liver mRNA levels of *Ghr* (growth hormone receptor) in *Zmpste24*$^{-/-}$ mice were lower than those found in WT animals, *Stat5a* (signal transducer and activator of transcription 5a) and *Socs2* (suppressor of cytokine signaling 2) mRNA levels were up-regulated in these progeroid mice (Fig. 2*B*). Although the functions of these two genes are antagonistic (*Socs2* down-regulates GH signaling, whereas *Stat5a* is one of the main transducers of this pathway), both genes are transcriptionally up-regulated in response to GH in the liver (22, 23). Therefore, the finding of increased mRNA levels for both factors in *Zmpste24*$^{-/-}$ progeroid mice is likely linked to the abnormally high circulating GH levels. Taken collectively, the transcriptional alterations in components of the somatotroph axis seen in *Zmpste24*$^{-/-}$ progeroid mice, together with the fact that *IGF-1* mRNA and protein levels remain reduced in presence of high circulating GH levels, point to a situation of GH resistance similar to that reported for some humans with Hutchinson–Gilford progeria (24). The finding that *Zmpste24*$^{-/-}$ male mice have very low levels of major urinary proteins (MUPs) (8) is also consistent with this situation, given that the synthesis of these proteins is dependent on somatotroph signaling (25, 26).

Considering the complexity of the somatotroph axis alterations found in *Zmpste24*$^{-/-}$ mice, we decided to evaluate in more detail the putative GH resistance observed in these progeroid animals. Thus, we analyzed the protein levels and relative phosphorylation of Jak2, Stat3, Stat5, and

Table 1. Liver transcriptome analysis of *Zmpste24*$^{-/-}$ reveals somatotroph axis transcriptional alterations

Gene name	Gene symbol	*Zmpste24*$^{-/-}$ vs. WT fold change
Signal transducer and activator of transcription 5B	*Stat5b*	7.55
IGF-binding protein 1	*Igfbp1*	6.37
Suppressor of cytokine signaling 3	*Socs3*	4.61
IGF-binding protein 3	*Igfbp3*	3.17
Suppressor of cytokine signaling 2	*Socs2*	2.20
Protein tyrosine phosphatase, nonreceptor type substrate 1	*Ptpns1*	2.09
Estrogen-related receptor, alpha	*Esrra*	1.84
Janus kinase 2	*Jak2*	1.28
Suppressor of cytokine signaling 1	*Socs1*	−1.28
Suppressor of cytokine signaling 5	*Socs5*	−1.41
Fibroblast growth factor receptor 4	*Fgfr4*	−1.52
Fibroblast growth factor 4	*Fgf4*	−1.67
Cytokine-inducible SH2-containing protein	*Cish*	−1.71
Insulin-like growth factor 1	*IGF-1*	−1.76
Growth hormone receptor	*Ghr*	−1.82
Insulin-like growth factor binding protein 5	*Igfbp5*	−1.98
Deiodinase, iodothyronine, type I	Dio1	−4.46
IGF-binding protein, acid labile subunit	Igfals	−7.24

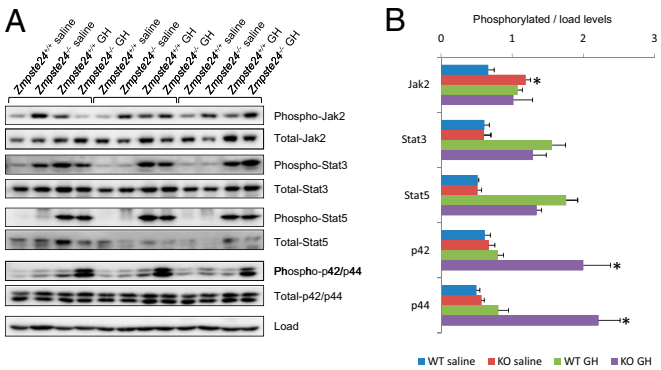

Fig. 2. GH-dependent transduction pathways analysis in *Zmpste24*$^{-/-}$ mice. Human recombinant GH was injected i.v. in overnight-fasted *Zmpste24*$^{+/+}$ and *Zmpste24*$^{-/-}$ mice. After 10 min, the mice were euthanized, and their livers were collected and flash-frozen. Liver response to GH was further analyzed by immunoblotting against major components of GH-induced signaling cascades. (*A*) Immunoblotting against total and phosphorylated forms of Jak2, Stat3, Stat5, and Erk1/2 in WT and *Zmpste24*$^{-/-}$ mice livers. (*B*) Densitometry analysis of the phosphorylated forms of GH-related signaling transducers shown in *A*. At least three WT and six mutant animals were used for each assay. $*P < 0.05$, two-tailed *t* test.

Erk1/2, all of which have been reported to be main effectors of GH stimulation (25), in response to i.v. GH injection. As shown in Fig. 2, stimulation with GH induced similar Jak2, Stat3, and Stat5 phosphorylation in the livers of both WT and *Zmpste24*$^{-/-}$ mice. However, whereas the GH-treated WT mice displayed only slight Erk1/2 activation, the GH-treated mutant mice exhibited strong phosphorylation of these proteins. Interestingly, we also found increased basal phosphorylation of Jak2 in *Zmpste24*$^{-/-}$ mice, which is consistent with the high levels of circulating GH in these animals. Conversely, basal phosphorylation levels of Stat3 and Stat5 were comparable in the mutant mice and WT livers. Taken together, these complex results indicate a nonuniform response among the multiple downstream effectors of GH and are likely a result of the multiple signaling alterations previously described in *Zmpste24*$^{-/-}$ mice (9, 17, 27). In this regard, the higher *Socs2* transcription levels displayed by mutant mice could specifically explain the absence of changes in Stat3 and Stat5, because Socs2 blocks the binding of Stat to GH receptor (28). Previous studies have shown that GH-mediated *IGF-1* transcription in vivo is dependent mainly on Stat5 activity (29); however, in vitro studies have shown that Mek inhibition stimulates *IGF-1* expression (30). Likewise, somatostatin has been reported to inhibit IGF-1 expression by activating the ERK-signaling pathway (31). Finally, the fact that human GH demonstrates a certain degree of lactogenic activity in mice must be considered (32). Thus, we cannot totally exclude the possibility that some of the complex and nonuniform signaling responses observed in progeroid mice after treatment with recombinant GH could be influenced by this phenomenon. Taken together, these results help explain the *IGF-1* mRNA down-regulation found in *Zmpste24*$^{-/-}$ mice. Nevertheless, it is likely that other signaling pathways also may contribute to the somatotroph axis changes seen in these mutant mice.

Additional signaling alterations, such as the previously described hyperactivation of p53 signaling (9) and down-regulation of the Wnt pathway (27), as well as the profound changes in glucose and lipid metabolism seen in *Zmpste24*$^{-/-}$ mice (18) might contribute to the observed decrease in *IGF-1* mRNA synthesis even in the presence of abnormally increased levels of circulating GH. Taking this into consideration, and given the increasing relevance of microRNAs (miRs) in the regulation of most physiological and pathological processes (33), we performed an exhaustive search of putative miRs predicted to target *IgfI*, because deregulation of miRs function could possibly help explain the observed paradoxical reduction in *IgfI* mRNA. Interestingly, we found that several miRs (miR-1, miR-26a and miR-27b) were predicted to target *IGF-1* (Fig. 3*A*). Consequently, we analyzed the transcriptional levels of these miRs in liver tissues from WT and progeroid mice. As shown in Fig. 3*A*, the expression levels of miR-26a and miR-27b in *Zmpste24*$^{-/-}$ mice liver tissues were similar to those seen in WT mice. In contrast, the expression of miR-1 was significantly higher in the liver, kidney, and muscle tissue of *Zmpste24*$^{-/-}$ mice compared with their WT littermates (Fig. 3*B*). Accordingly, we decided to analyze in more detail whether or not miR-1 is able to repress IGF-1. For this, we performed luciferase assays using a fusion of the 3′-UTR of murine *IgfI* downstream of the cDNA of Renilla luciferase. As shown in Fig. S1, we confirmed a functional binding site for miR-1 in the 3′-UTR of *IGF-1*. In addition, a 2-nt substitution in the putative seed sequence of miR-1 was sufficient to significantly reduce miR-1 repressive effect over the 3′-UTR of *IGF-1*, thus confirming that *IGF-1* is a bona fide target for miR-1. During the preparation of this manuscript, and consistent with our findings, it has been reported that miR-1 is able to target *IGF-1* in the context of cardiac and skeletal muscle physiology (34, 35), which supports our results. To further examine this putative link among miR-1, IGF-1, and progeroid syndromes, we analyzed miR-1 expression levels in cultured fibroblasts derived from patients with Hutchinson–Gilford progeria syndrome. As shown in Fig. 3*C*, these human progeroid cells also exhibited a marked transcriptional up-regulation of miR-1 compared with control fibroblasts. Interestingly, cultured murine fibroblasts subjected to persistent DNA damage also exhibited increased miR-1 mRNA levels (Fig. 3*D*). This finding also agrees with previous reports of reduced *IGF-1* expression in WT mice exposed to a low dose of chronic genotoxic stress (36), as well as with the fact that cells from both Hutchinson–Gilford progeria patients and *Zmpste24*$^{-/-}$ mice show increased DNA damage (37). Taken together, these findings suggest that miR-1 up-regulation occurs in both progeroid mice and human Hutchinson–Gilford progeria cells and likely contributes to somatotroph axis suppression by reducing IGF-1 synthesis, even in the presence of elevated circulating GH levels.

Finally, in this work we explored whether the detailed characterization of the somatotroph axis alterations observed in *Zmpste24*$^{-/-}$ mice could lead to the development of therapeutic strategies for human progeroid syndromes. We decided to first evaluate the effect of recombinant human IGF-1 (rIGF-1) treatment on *Zmpste24*$^{-/-}$ mice to test whether somatotroph axis restoration could ameliorate or aggravate their progeroid phenotype, including their reduced longevity. To provide continuous rIGF-1 delivery, we used subcutaneous osmotic pumps, which ensure uniform drug delivery into the systemic circulation. The successful delivery of rIGF-1 was further verified by ELISA analysis of human IGF-1 levels in treated mice (Fig. 4). Interestingly, *Zmpste24*$^{-/-}$ mice treated with rIGF-1 demonstrated substantial recovery of progeroid phenotypes (Fig. 4). Thus, rIGF-1 treatment improved body weight, increased the amount of subcutaneous fat, reduced the degree of kyphosis and alopecia, and significantly extended the longevity of *Zmpste24*$^{-/-}$ mice ($P = 0.025$, log-rank test) (Fig. 4). The median survival of treated *Zmpste24*$^{-/-}$ mice was extended from 123 d to 145 d, and the maximum survival was extended from 151 d to 187 d. Notably, all phenotypes rescued in *Zmpste24*$^{-/-}$ progeroid mice represent characteristic features of Hutchinson–Gilford progeria in humans. Moreover, 4-mo-old rIGF-1–treated mice had similar GH levels as WT mice, whereas age-matched saline-treated progeroid mice had dramatically increased circulating GH levels, suggesting that rIGF-1 treatment restored the observed somatotroph axis alterations of *Zmpste24*$^{-/-}$ mice. In fact, the 4-mo-old treated mice had normal MUP concentrations in urine (Fig. 4), providing additional support to the restoration of the GH/IGF-1 function in mutant mice treated with rIGF-1.

Discussion

In recent years, the effect of somatotroph axis alterations on lifespan extension has been a subject of extensive analysis (38). The first evidence pointing to a longevity regulatory role of IGF-1 signaling was reported in nematodes. In fact, worms lacking *Daf2*, the ortholog of mammalian insulin/IGF-1 receptor, have a dramatically increased lifespan (39). Similarly, flies harboring inactivating mutations in *InR* (the ortholog of *C. elegans Daf2* and mammalian *IR* and *IGF-1R*) have

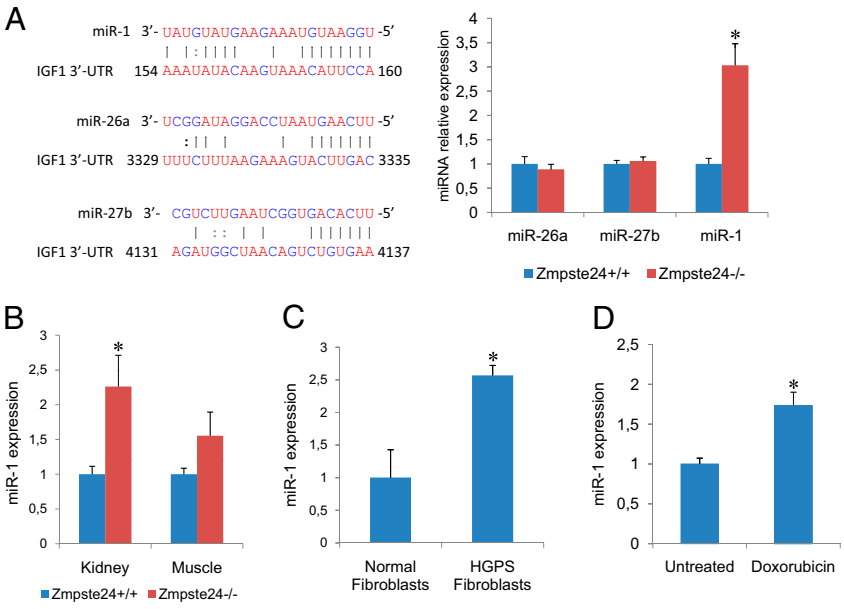

Fig. 3. miR-1 expression analysis in *Zmpste24*$^{-/-}$ mice and Hutchinson–Gilford progeria cells. (*A*) qPCR analysis of putative IGF-1 microRNAs. A selection of TargetScan-predicted microRNAs targeting IGF-1 (*Left*) were analyzed by qPCR in liver samples (*Right*) from WT (blue bars) and *Zmpste24*$^{-/-}$ mice (red bars). (*B*) miR-1 expression studies were extended to the indicated tissues from WT and *Zmpste24*$^{-/-}$ mice. (*C*) miR-1 expression levels in in human fibroblasts from patients with Hutchinson–Gilford progeria syndrome. (*D*) miR-1 expression levels in WT fibroblasts untreated and treated with 0.5 μM doxorubicin for 24 h.

a significantly increased lifespan (40). In mammals, both reduced insulin and IGF-1 signaling are commonly found in long-lived organisms. Thus, a reduction in IGF-1 signaling alone is sufficient to significantly extend the lifespan, at least in mice (41). More surprisingly, a pathological condition such as LS, which is associated with GH resistance and growth retardation, extends longevity in mice and confers some degree of cancer protection in humans (42). Notably, and despite their reduced growth rate and body size, LS mice exhibit reduced circulating IGF-1 levels and increased blood GH content and greater longevity compared with control animals (43). Thus, the finding that *Zmpste24*$^{-/-}$ progeroid mice present features of GH resistance similar to those seen in LS mice, as well as additional alterations associated with lifespan extension, such as increased autophagy (17), is both paradoxical and intriguing.

Previous reports have noted a number of unexpected similarities between phenotypic alterations found in murine models of premature aging and long-lived organisms, including reduced circulating IGF-1 levels (36, 44, 45). All these alterations seem to be part of an adaptive stress response aimed at preserving organism viability under compromising circumstances (14, 15). These features common to both long-lived and premature-aged individuals have been proposed to arise from a progressive and age-dependent accumulation of DNA damage, which is highly exacerbated in progeroid syndromes (46). In addition, DNA damage induction in vivo has been shown to lead to a series of alterations similar to those observed in both progeroid and long-lived animals (14, 44). Thus, it seems reasonable that long-lived organisms that have been able to overcome cancer, cardiovascular, or other life-threatening pathologies accumulate DNA damage with aging that eventually elicits an adaptive stress response similar to that observed at an early age in progeroid individuals. This response is aimed at reallocating resources from growth to somatic preservation, given that normal growth or proliferation rates in cells that accumulate a critical amount of DNA damage will unequivocally lead to replication defects, chromosomal instability, nuclear envelope abnormalities, and, finally, the development of cancer (15). It is tempting to speculate that if this putative adaptive response fails to counteract the detrimental effects of DNA damage accumulation, then progeroid mice will finally succumb to cancer. Conversely, if this strategy is successful, then progeroid mice that have acquired features of long-lived organisms will exhibit reduced metabolic and growth rates, but not the characteristic lifespan reduction. This could be due to overactivation of antiproliferative pathways induced by the massive accumulation of DNA damage, which leads to a systemic senescent state and finally to premature death. The somatotroph axis alterations found in *Zmpste24*$^{-/-}$ progeroid mice could constitute a clear example of redundant oversuppression of a growth-

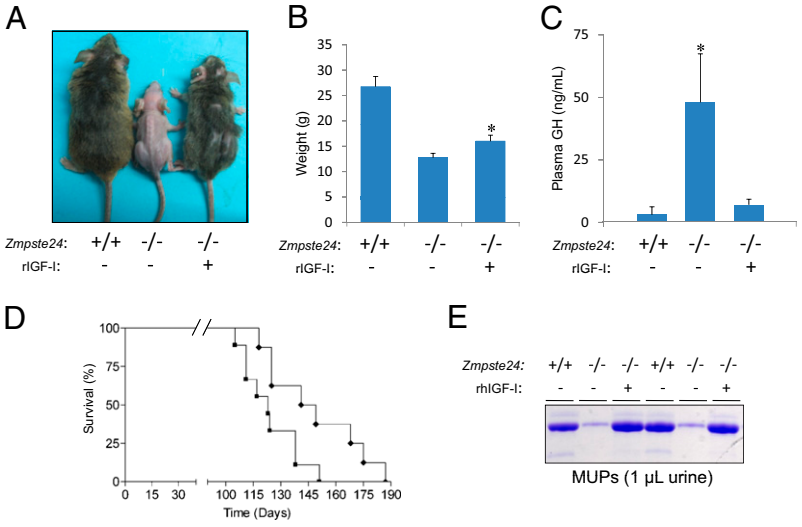

Fig. 4. Recombinant IGF-1 treatment ameliorates *Zmpste24*-deficient mice progeroid phenotypes. (*A*) Representative photographs of 4-mo-old *Zmpste24*$^{+/+}$ and *Zmpste24*$^{-/-}$ mice untreated and treated with recombinant human IGF-1. (*B*) Total body weight of 3-mo-old *Zmpste24*$^{+/+}$ ($n = 6$), *Zmpste24*$^{-/-}$ ($n = 8$), and treated *Zmpste24*$^{-/-}$ ($n = 8$) mice. The treated mice exhibit a significant recovery of the total body weight. (*C*) Recombinant IGF-1 treatment restores GH levels of 4-mo-old *Zmpste24*$^{-/-}$ mice to those observed in their age-matched WT littermates. (*D*) Kaplan-Meier graph showing a significant increment of the maximum life span in IGF-1–treated *Zmpste24*$^{-/-}$ mice (diamonds; $n = 8$) compared with untreated mice (squares; $n = 8$). (*E*) Representative SDS/PAGE gel showing normal MUPs urine content in 4-mo-old *Zmpste24*$^{-/-}$ mice treated with recombinant IGF-1.

promoting pathway. In fact, progeroid mice show alterations in multiple regulators of GH-mediated signaling, including up-regulation of *Socs2* and *Igfbp1* together with down-regulation of *Igfl*, *Igfals*, and *Ghr* genes, clearly pointing to an strategy of growth suppression. Moreover, the marked up-regulation of miR-1 observed in both *Zmpste24*$^{-/-}$ mice and Hutchinson-Gilford Progeria syndrome cells likely contributes to the exacerbated suppression of liver IGF-1 synthesis observed in progeroid mice, even in the presence of high circulating GH levels.

The possibility that the dramatically increased circulating GH levels could constitute one of the main determinants of the premature aging of *Zmpste24*$^{-/-}$ mice should be considered as well. In fact, although progeroid mice demonstrate liver GH resistance in terms of IGF-1 synthesis, they show no significant alteration in Jak/Stat pathway activation after i.v. GH injection. Thus, it is possible that the observed supraphysiological circulating GH levels could directly elicit a variety of detrimental responses in peripheral tissues, which could contribute to the development of premature aging. Interestingly, liver-specific knockout mice with reduced IGF-1 and increased GH circulating levels exhibited metabolic defects that could be corrected by the administration of a GH antagonist (47). This demonstrates that high levels of circulating GH can be detrimental and contribute to a shortened lifespan. Moreover, giant GH transgenic mice were found to have several features of accelerated aging (48), supporting the idea that the increased GH levels in *Zmpste24*$^{-/-}$ mice could contribute to the organismal wasting that accompanies accelerated aging. In contrast, the increased longevity seen in LS mice indicates that somatotroph axis-linked regulation of longevity is precisely fine-tuned. Consistently, our finding that rIGF-1 administration extends longevity and ameliorates several progeroid features of *Zmpste24*$^{-/-}$ mice suggests that the intensity of the systemic adaptive response seen in premature aging conditions is excessive and must be modulated to extend longevity. Thus, although the complete elimination of the antiproliferative alterations observed in progeroid mice would likely result in cancer, the selective modification of some signaling pathways in these mice could be beneficial for extending longevity. Accordingly, we have previously shown that a reduction in p53 signaling delays the onset of progeroid features and increases the lifespan in *Zmpste24*$^{-/-}$ mice (9). Our observation that rIGF-1–mediated restoration of somatotroph axis status—altered in both accelerated aging models and some progeria patients (24, 45)—extends longevity in mice points in the same direction. IGF-1 has proven effective in treating GH-refractory somatotroph alterations in humans with no significant detrimental effects (49). Accordingly, rIGF-1 treatment, alone or in combination with other drugs, such as statins and bisphosphonates (50), merits exploration as a therapeutic approach to slow disease progression in children with progeria.

Materials and Methods

Transgenic Animals. Mutant mice deficient in Zmpste24 metalloproteinase have been described previously (8). All animal experiments were conducted in accordance with the guidelines of the University of Oviedo's Committee on Animal Experimentation.

Recombinant IGF-1 Administration. Mice were treated with recombinant human IGF-1 (Prospec) at a daily dose of 1 mg/kg of body mass. IGF-1 dissolved in 10 mmol/L of HCl and sterile isotonic saline at a concentration of 8.3 mg/mL was loaded into a miniosmotic pump (model 1004; Alzet) that had a pumping rate of 0.125 μL/h (3 μL/d) for 28 d. Loaded pumps were primed in isotonic saline at 37 °C for 24 h before implantation. Mice assigned to receive IGF-1 were anesthetized with isoflurane such that they were unresponsive to tactile stimuli, whereupon an incision was made in the skin in the middle of the spinal curvature and an s.c. pocket was created via blunt dissection with surgical scissors. Pumps were inserted into the s.c. space with the flow regulator cap directed distally, and the incision was closed with Michel clips. After 28 d of continuous IGF-1 administration, the pumps were replaced with freshly loaded and primed units to enable a further 28 d of treatment by the same procedure. On removal, the pumps were aspirated to ensure that fouling had not occurred and that the contents had been administered appropriately.

Immunoblot Analysis. After extraction, mouse tissues were immediately frozen in liquid nitrogen and then homogenized in a 20 mM Tris buffer (pH 7.4) containing 150 mM NaCl, 1% Triton X-100, and 10 mM EDTA, Complete Protease Inhibitor Mixture (Roche Applied Science), and phosphatase inhibitors (200 μM sodium orthovanadate, 1 mM β-glycerophosphate). Once homogenized, tissue extracts were centrifuged at 12,000 × *g* and 4 °C, and supernatants were collected. Supernatant protein concentration was evaluated by the bicinchoninic acid technique (Pierce BCA Protein Assay Kit). Then 25 μg of each protein sample was loaded onto 8% SDS-polyacrylamide gels. After electrophoresis, the gels were electrotransferred onto nitrocellulose filters, and the filters were then blocked with 5% nonfat dried milk in PBT (PBS with 0.05% Tween 20) and incubated with primary antibodies in 5% BSA in PBT. After three washes with PBT, filters were incubated with HRP-conjugated goat anti-rabbit IgG at a 1:10,000 dilution in 1.5% milk in PBT, and developed with a West Pico enhanced chemiluminescence kit (Pierce). All of the antibodies used in this work were obtained from Cell Signaling.

Blood and Plasma Parameters. The mice were starved for 5 h to avoid any possible alteration in blood parameters due to food intake before measurements. After the mice were anesthetized with isoflurane, blood was extracted directly from the heart. Plasma was obtained as described previously (17). In brief, blood was centrifuged immediately after collection at 3,000 × *g* and 4 °C, and the supernatant was collected and stored at −70 °C until analysis. Plasma IGF-1 concentration was determined using the R&D Systems Quantikine ELISA kit, whereas plasma GH concentration was measured using the Linco ELISA kit, according to the manufacturer's instructions.

RNA Preparation. Collected tissue was immediately homogenized in TRIzol reagent (Invitrogen) and processed on the same day through alcohol precipitation. RNA pellets were then washed in cold 80% ethanol and stored at −80 °C until further use. After resuspension of RNA in nuclease-free water (Ambion), the samples were quantified and evaluated for purity (260 nm/280 nm ratio) using a NanoDrop ND-1000 spectrophotometer, and 100 μg of each sample was further purified using Qiagen RNeasy spin columns according to the manufacturer's instructions.

Analysis of Liver Response to GH Injection. Recombinant human GH was injected i.v. with a 5 mg/kg dose in 3.5-mo-old *Zmpste24* WT and KO mice fasted overnight. At 10 min after GH injection, the mice were killed, and their livers were collected and flash-frozen in liquid nitrogen. Liver response to GH was analyzed by immunoblotting using antibodies against major components of GH-induced signaling cascades.

Quantitative RT-PCR Analysis. cDNA was synthesized using 1–5 μg of total RNA, 0.14 mM oligo(dT) (22-mer) primer, 0.2 mM concentrations of each dNTP, and SuperScript II reverse transcriptase (Invitrogen). Quantitative RT-PCR (qRT-PCR) was carried out in triplicate for each sample using 20 ng of cDNA, TaqMan Universal PCR Master Mix (Applied Biosystems), and 1 μL of the specific TaqMan custom gene expression assay for the gene of interest (Applied Biosystems). To quantify gene expression, PCR was performed at 95 °C for 10 min and at 50 °C for 2 min, followed by 40 cycles of 95 °C for 15 s and 60 °C for 1 min, using an Applied Biosystems 7300 real-time PCR system. As an internal control for the amount of template cDNA used, gene expression was normalized to the mouse β-actin gene using the mouse β-actin endogenous control (VIC/MGB probe; primer limited) TaqMan gene expression assay (Applied Biosystems). Relative expression of the distinct analyzed genes was calculated according to the manufacturer's instructions. In brief, the analyzed gene expression was normalized to β-actin in WT or *Zmpste24*$^{-/-}$ derived samples, using the following formula: the mean values of $2^{\Delta CTgene\ (gene\ of\ interest)-\Delta CTgene\ (\beta\text{-}actin)}$ for at least six different WT animals were considered 100% for each analyzed gene, and the same values for *Zmpste24*$^{-/-}$ mice tissues were referred to those values, as described previously (51).

Luciferase Assays. Computational prediction of the conserved miR-binding sites in the mouse *IGF-1* 3′-UTR was carried out using TargetScan software (http://www.targetscan.org). The entire 3′-UTR sequence of *IGF-1* was cloned into psiCHECK-2 plasmid (Promega) downstream of the Renilla luciferase ORF using the restriction enzymes XhoI and NotI. HEK-293 cells were seeded 6 h before transfection in 24-well plates at 50% of confluence in growth media without antibiotics. Tranfections were performed using Lipofectamine 2000 (Invitrogen), 250 ng of each psiCHECK-2 construct, and 20 pmol of miR-1 or control miR molecules (Ambion), following the manufacturer's instructions. Transfection was carried out for 4 h, after which the medium was removed and cells were left to recover for 18 h. Luciferase activity was measured using the Promega Dual-Luciferase Reporter Assay System. In brief, cells on 24-well plates were washed with PBS and lysed by pipetting up and down in the well using 80 μL of the passive lysis buffer. Then both Renilla (reporter gene) and

firefly (endogenous control) luciferase activity of each sample were measured in a Turner Biosystems TD-20/20 luminometer. Each assay was carried out in triplicate, and Renilla activity was normalized to the firefly activity detected in the same sample.

miRNA analysis. Total RNA was prepared using the Ambion miRVANA miRNA Isolation Kit, and RNA samples were quantified and evaluated for purity (260 nm/280 nm ratio) using a NanoDrop ND-1000 spectrophotometer. miRNA detection was performed using TaqMan miRNA expression assays (Applied Biosystems). In brief, 10 ng of total RNA was reverse-transcribed using the TaqMan miRNA Reverse-Transcription Kit (Applied Biosystems) and PCR-amplified using the Applied Biosystems 7300 Real-Time PCR System. As an internal control, miRNA expression was normalized to snoRNA202 for mouse samples and to RNU6B for human samples, using TaqMan Gene Expression Assays (Applied Biosystems). All of the protocols were carried out according to the manufacturer's instructions.

Cell Culture. Human Hutchinson–Gilford progeria syndrome cells (AG11498) were obtained from the Coriell Cell Repository. Cultures were maintained in DMEM (Gibco) supplemented with 10% FBS and 1% penicillin-streptomycin-glutamine (Gibco). Murine fibroblasts were extracted from 12-wk-old mice ears. The ears were sterilized with ethanol, washed with PBS, and triturated with razor blades. The resulting samples were incubated with 600 μL of 4-mg/mL collagenase D (Roche) and 4 mg/mL of dispase II (Roche) in DMEM for 45 min in 5% CO_2 at 37 °C. After filtering and washing, 6 mL of DMEM with 10% FBS and 1% antibiotic-antimycotic were added, and the mixture was incubated in 5% CO_2at 37 °C. Approximately 10^6 cells were passed in a 10-cm plate every 3 d and cultured under standard conditions. For DNA damage induction, murine fibroblasts were seeded in six-well plates; after 24 h, doxorubicin (Sigma-Aldrich) was added to the growing media at 0.5 μM, and 24 h later, RNA was extracted and miR-1 expression analyzed.

Statistical Analysis. All experimental data are reported as means; error bars represent SEM. Statistical analysis was performed with the nonparametric Student *t* test using GraphPad Prism version 4.0. Kaplan-Meier survival analysis was performed using the MedCalc statistical package.

ACKNOWLEDGMENTS. We thank Drs. A. Astudillo and A. J. Ramsay for helpful comments and F. Rodríguez, S. Álvarez, M. Fernández, and D. Álvarez for excellent technical assistance. This work was supported by grants from Ministerio de Ciencia e Innovación-Spain, Fundación "M. Botín," and European Union (FP7 MicroEnviMet). The Instituto Universitario de Oncología is supported by Obra Social Cajastur and Acción Transversal del Cáncer-Red Temática de Investigación Cooperativa en Cáncer.

1. Kirkwood TB (2005) Understanding the odd science of aging. *Cell* 120:437–447.
2. Vijg J, Campisi J (2008) Puzzles, promises and a cure for ageing. *Nature* 454:1065–1071.
3. Ramírez CL, Cadiñanos J, Varela I, Freije JM, López-Otín C (2007) Human progeroid syndromes, aging and cancer: New genetic and epigenetic insights into old questions. *Cell Mol Life Sci* 64:155–170.
4. Hennekam RC (2006) Hutchinson–Gilford progeria syndrome: Review of the phenotype. *Am J Med Genet A* 140:2603–2624.
5. Kudlow BA, Kennedy BK, Monnat RJ, Jr. (2007) Werner and Hutchinson–Gilford progeria syndromes: Mechanistic basis of human progeroid diseases. *Nat Rev Mol Cell Biol* 8:394–404.
6. Pereira S, et al. (2008) HGPS and related premature aging disorders: From genomic identification to the first therapeutic approaches. *Mech Ageing Dev* 129:449–459.
7. Gruenbaum Y, Margalit A, Goldman RD, Shumaker DK, Wilson KL (2005) The nuclear lamina comes of age. *Nat Rev Mol Cell Biol* 6:21–31.
8. Pendás AM, et al. (2002) Defective prelamin A processing and muscular and adipocyte alterations in Zmpste24 metalloproteinase-deficient mice. *Nat Genet* 31:94–99.
9. Varela I, et al. (2005) Accelerated ageing in mice deficient in Zmpste24 protease is linked to p53 signalling activation. *Nature* 437:564–568.
10. Osorio FG, Obaya AJ, López-Otín C, Freije JM (2009) Accelerated ageing: From mechanism to therapy through animal models. *Transgenic Res* 18:7–15.
11. Bergo MO, et al. (2002) *Zmpste24* deficiency in mice causes spontaneous bone fractures, muscle weakness, and a prelamin A processing defect. *Proc Natl Acad Sci USA* 99:13049–13054.
12. Sullivan T, et al. (1999) Loss of A-type lamin expression compromises nuclear envelope integrity leading to muscular dystrophy. *J Cell Biol* 147:913–920.
13. Russell SJ, Kahn CR (2007) Endocrine regulation of ageing. *Nat Rev Mol Cell Biol* 8: 681–691.
14. Garinis GA, et al. (2009) Persistent transcription-blocking DNA lesions trigger somatic growth attenuation associated with longevity. *Nat Cell Biol* 11:604–615.
15. Hoeijmakers JH (2009) DNA damage, aging, and cancer. *N Engl J Med* 361:1475–1485.
16. Laron Z (2004) Laron syndrome (primary growth hormone resistance or insensitivity): The personal experience 1958–2003. *J Clin Endocrinol Metab* 89:1031–1044.
17. Mariño G, et al. (2008) Premature aging in mice activates a systemic metabolic response involving autophagy induction. *Hum Mol Genet* 17:2196–2211.
18. Mariño G, López-Otín C (2008) Autophagy and aging: New lessons from progeroid mice. *Autophagy* 4:807–809.
19. Ueki I, et al. (2000) Inactivation of the acid labile subunit gene in mice results in mild retardation of postnatal growth despite profound disruptions in the circulating insulin-like growth factor system. *Proc Natl Acad Sci USA* 97:6868–6873.
20. Domené HM, Bengolea SV, Jasper HG, Boisclair YR (2005) Acid-labile subunit deficiency: Phenotypic similarities and differences between human and mouse. *J Endocrinol Invest* 28 (5):Suppl):43–46.
21. Gay E, et al. (1997) Liver-specific expression of human insulin-like growth factor binding protein-1 in transgenic mice: Repercussions on reproduction, ante- and perinatal mortality and postnatal growth. *Endocrinology* 138:2937–2947.
22. Ortiz BL, Sánchez-Gómez M, Norstedt G (2000) Comparison of STAT5 mRNA levels in GH-treated male and female rats analysed by a solution hybridization assay. *Growth Horm IGF Res* 10:236–241.
23. Tollet-Egnell P, Flores-Morales A, Stavréus-Evers A, Sahlin L, Norstedt G (1999) Growth hormone regulation of SOCS-2, SOCS-3, and CIS messenger ribonucleic acid expression in the rat. *Endocrinology* 140:3693–3704.
24. Abdenur JE, Brown WT, Friedman S, Smith M, Lifshitz F (1997) Response to nutritional and growth hormone treatment in progeria. *Metabolism* 46:851–856.
25. Rowland JE, et al. (2005) In vivo analysis of growth hormone receptor signaling domains and their associated transcripts. *Mol Cell Biol* 25:66–77.
26. Norstedt G, Palmiter R (1984) Secretory rhythm of growth hormone regulates sexual differentiation of mouse liver. *Cell* 36:805–812.
27. Espada J, et al. (2008) Nuclear envelope defects cause stem cell dysfunction in premature-aging mice. *J Cell Biol* 181:27–35.
28. Flores-Morales A, Greenhalgh CJ, Norstedt G, Rico-Bautista E (2006) Negative regulation of growth hormone receptor signaling. *Mol Endocrinol* 20:241–253.
29. Barclay JL, et al. (2010) In vivo targeting of the growth hormone receptor (GHR) Box1 sequence demonstrates that the GHR does not signal exclusively through JAK2. *Mol Endocrinol* 24:204–217.
30. Frost RA, Nystrom GJ, Lang CH (2002) Regulation of IGF-1 mRNA and signal transducers and activators of transcription-3 and -5 (Stat-3 and -5) by GH in C2C12 myoblasts. *Endocrinology* 143:492–503.
31. Hagemeister AL, Sheridan MA (2008) Somatostatin inhibits hepatic growth hormone receptor and insulin-like growth factor I mRNA expression by activating the ERK and PI3K signaling pathways. *Am J Physiol Regul Integr Comp Physiol* 295:R490–R497.
32. Fuh G, Colosi P, Wood WI, Wells JA (1993) Mechanism-based design of prolactin receptor antagonists. *J Biol Chem* 268:5376–5381.
33. Bushati N, Cohen SM (2007) MicroRNA functions. *Annu Rev Cell Dev Biol* 23:175–205.
34. Shan ZX, et al. (2009) Up-regulated expression of miR-1/miR-206 in a rat model of myocardial infarction. *Biochem Biophys Res Commun* 381:597–601.
35. Elia L, et al. (2009) Reciprocal regulation of microRNA-1 and insulin-like growth factor-1 signal transduction cascade in cardiac and skeletal muscle in physiological and pathological conditions. *Circulation* 120:2377–2385.
36. van der Pluijm I, et al. (2007) Impaired genome maintenance suppresses the growth hormone—insulin-like growth factor 1 axis in mice with Cockayne syndrome. *PLoS Biol* 5:e2.
37. Liu B, et al. (2005) Genomic instability in laminopathy-based premature aging. *Nat Med* 11:780–785.
38. Bartke A (2005) Minireview: Role of the growth hormone/insulin-like growth factor system in mammalian aging. *Endocrinology* 146:3718–3723.
39. Kenyon C, Chang J, Gensch E, Rudner A, Tabtiang R (1993) A *C. elegans* mutant that lives twice as long as wild type. *Nature* 366:461–464.
40. Tatar M, et al. (2001) A mutant *Drosophila* insulin receptor homolog that extends life span and impairs neuroendocrine function. *Science* 292:107–110.
41. Holzenberger M, et al. (2003) IGF-1 receptor regulates lifespan and resistance to oxidative stress in mice. *Nature* 421:182–187.
42. Laron Z (2008) The GH-IGF-1 axis and longevity: The paradigm of IGF-1 deficiency. *Hormones (Athens)* 7:24–27.
43. Coschigano KT, et al. (2003) Deletion, but not antagonism, of the mouse growth hormone receptor results in severely decreased body weights, insulin, and insulin-like growth factor I levels and increased life span. *Endocrinology* 144:3799–3810.
44. Niedernhofer LJ, et al. (2006) A new progeroid syndrome reveals that genotoxic stress suppresses the somatotroph axis. *Nature* 444:1038–1043.
45. van de Ven M, et al. (2006) Adaptive stress response in segmental progeria resembles long-lived dwarfism and calorie restriction in mice. *PLoS Genet* 2:e192.
46. Garinis GA, van der Horst GT, Vijg J, Hoeijmakers JH (2008) DNA damage and ageing: New-age ideas for an age-old problem. *Nat Cell Biol* 10:1241–1247.
47. Yakar S, et al. (2004) Inhibition of growth hormone action improves insulin sensitivity in liver IGF-1–deficient mice. *J Clin Invest* 113:96–105.
48. Wolf E, et al. (1993) Effects of long-term elevated serum levels of growth hormone on life expectancy of mice: Lessons from transgenic animal models. *Mech Ageing Dev* 68: 71–87.
49. Clemmons DR (2007) Modifying IGF-1 activity: An approach to treat endocrine disorders, atherosclerosis and cancer. *Nat Rev Drug Discov* 6:821–833.
50. Varela I, et al. (2008) Combined treatment with statins and aminobisphosphonates extends longevity in a mouse model of human premature aging. *Nat Med* 14:767–772.
51. Livak KJ, Schmittgen TD (2001) Analysis of relative gene expression data using real-time quantitative PCR and the 2(-Delta Delta C(T)) method. *Methods* 25:402–408.